A comparative study of the wave energy collected at Saint Jean de Luz (France) by an overtopping converter and a flap activated converter

Mathieu Mory, Jérémy Dugor, V. Baudry, Aurélien Babarit, Alain H. Clément

A comparative study of the wave energy collected at Saint Jean de Luz (France) by an overtopping converter and a flap activated converter (20°)

M. Mory[#1], J. Dugor[*2], V. Baudry[§3], A. Babarit[§4]& A.H. Clément[§5]

[#]*SIAME, Université de Pau et des Pays de l'Adour, BP 7511, 64075 PAU Cédex, France*

[1]mathieu.mory@univ-pau.fr

[*]*Casagec Ingénierie, 4 route de Pitoys, 64600 ANGLET, France*

[2]dugor@casagec.fr

[§] *Ecole Centrale de Nantes, LHEEA (ECN/CNRS),*
1 rue de la Noé, BP 92101, 44321 Nantes Cédex 3, France

[3]virginie.baudry@ec-nantes.fr

[4]Aurelien.Babarit@ec-nantes.fr

[5]alain.clement@ec-nantes.fr

***Abstract*—An overtopping wave energy converter and a flap-type wave energy converter are considered for implementation in front of a coastal structure protecting the bay of Saint Jean de Luz. The wave energy resource and the tidal conditions are first determined. The energy recovered by the two converters is subsequently estimated for different design and/or conditions of operations. An optimized design is proposed for the overtopping wave energy converter with a five levels reservoir. For the flap converter, the study investigates the optimization of the Power Take-Off (PTO) parameters, in order to maximize the energy recovered. The choice of PTO parameters is primarily guided by the requirement that the motion amplitude of the flap should remain within an acceptable range for all wave and tidal conditions.**

***Keywords*— Wave energy, wave flap converter, wave overtopping converter, control, site study**

I. Introduction

In the southwest along the Atlantic coast of France, Saint Jean de Luz is a well known place for its intense wave climate. The monthly averaged offshore wave power ranges from 10 kW/m in summer to 80 kW/m in winter. The coastal area is therefore gaining attention for the possible implementation of wave energy converters.

This design study was partially funded by the EMACOP project (France), which aims at studying the feasibility and relevance of combining wave energy converters with coastal protection structures. Sharing the civil engineering costs of marine energy systems and coastal defence structures could provide a global economic benefit, enhancing the interest of port and coastal authorities and investors for wave power systems.

Recovering wave energy has inspired engineers since more than a hundred years but the literature on the subject increased markedly since 1980. The recent review by Falcão [1] indicates that more than one thousand patents have been registered. The numerous technologies for recovering wave energy are classified [1] into three categories: i. Oscillating Water Column (OWC) systems, where waves compress the air in a closed chamber and energy is recovered using an air turbine; ii. Bodies oscillating under the action of waves, which activate an electrical converter; iii. Overtopping systems, which recover the potential energy of overtopping waves using a low-head hydraulic turbine. Up to now, few full-scale prototypes have been built. We mention the recent OWC system at Mutriku [2]. The location is close from Saint Jean de Luz and the system operates for similar wave conditions. As addressed by the EMACOP program, the Mutriku project aimed at combining wave energy recovery to a coastal defence issue.

The bay at Saint Jean de Luz is protected by three dikes. The paper presents a comparative study of the wave energy potentially collected by two energy converters located in front of the so-called Artha dike:

- An overtopping wave energy converter: the geometry of a Sea-wave Slot-cone Generator (SSG) was chosen, for the design of this technology is well documented [3-6],
- A flap-type oscillating wave converter [7], for which numerical models are available [8].

This study aims at predicting the average power that could be recovered by the two systems. The power matrices were determined for varying significant wave height H_s and wave period T_p at the location of the converters and varying water depth h to account for the tide. The average power recovered was then estimated using the probability of wave occurrence.

The study identifies the wave and tidal conditions that contribute to significant energy recovery. In view of the results, designs for the two systems are proposed. The design of the SSG system fixes the number of reservoirs and their crest heights. The geometric design of the flap-type wave energy converter is coupled with the selection of optimum Power Take Off (PTO) parameters.

The focus of the paper is on the conversion of wave energy into the mechanical energy recovered by the wave energy converters (WEC). The results presented are preliminary. They cannot not be used to compare the economical performance of the two WEC technologies since energy losses of turbines, electrical converters, etc, are not taken into account. This is further discussed in the conclusion.

The paper is divided in five sections. Section II is devoted to the site description and the locations for implementing the wave converters are discussed. Section III presents the results of simulations of wave propagation from offshore and describes the wave and tidal conditions at the locations of the wave converters. Sections IV and V present the results on the energy recovery by the SSG overtopping converter and by the oscillating flap converter, respectively, and discuss their optimized designs. Section VI is the conclusion.

II. Site Description

Saint Jean de Luz is located on the French Atlantic coast, close to the Spanish border. The bay is sheltered by three breakwaters (Fig. 1) named from West to East: Socoa, Artha and Sainte Barbe.

A serie of 10 points have been chosen in the vicinity of the three dikes along the isobath -4m below the lowest tidal level. The wave energy potential has been determined (see section III) at these 10 points in order to select the best location for installing a wave energy converter. Due to a rocky reef, the -4 m isobath is located a few tens of meters offshore from the Socoa and Sainte Barbe dikes.

The seabed slope is much steeper in front of Artha and at the end of Socoa breakwater. The isobath -4 m along the Artha dike is close to the structure. Considering the interesting wave energy potential and the implementation convenience, the point P7, located in front of the middle of the Artha dike, has been selected for the possible implementation of the two wave energy converters. The implementation of converters was studied at a location position where the sea bottom is h_0=8m below the lowest tidal level.

III. Wave Climate Conditions

A. Method

The wave climate in front of the Artha dike was determined from numerical simulations of wave propagation from offshore into the bay of Saint Jean de Luz, using the SWAN model of Delft University [9]. The wave forcing was achieved using wave data (significant wave height H_s, wave period T_p, direction of propagation and directional spread) known at three points labelled OCEAN 1563, OCEAN 1566 and OCEAN 1569. Fig. 2 shows the simulation domain and the locations of the three points in its north boundary. The forcing wave data were extracted from the ANEMOC data base which covers a duration of 23.5 years (01/01/1979 to 31/08/2002) on the Atlantic French coast [10]. Wave simulations were carried out in three nested grids shown in Fig. 2, with grid cells of approx. 800m in the full domain, approx. 200m in the intermediate domain (red rectangle) and approx. 20m in the smaller domain (blue rectangle), where Saint Jean de Luz is located. The quality of significant wave height predictions in the vicinity of the coast has been checked by a comparison with the ANEMOC data at the three points COAST 0011, COAST 0016 and COAST 2397 (indicated in Fig. 2). The agreement is good. The root mean square error on the significant wave height is below 15 cm at the two points in the North and equal to 33 cm at the point C2397.

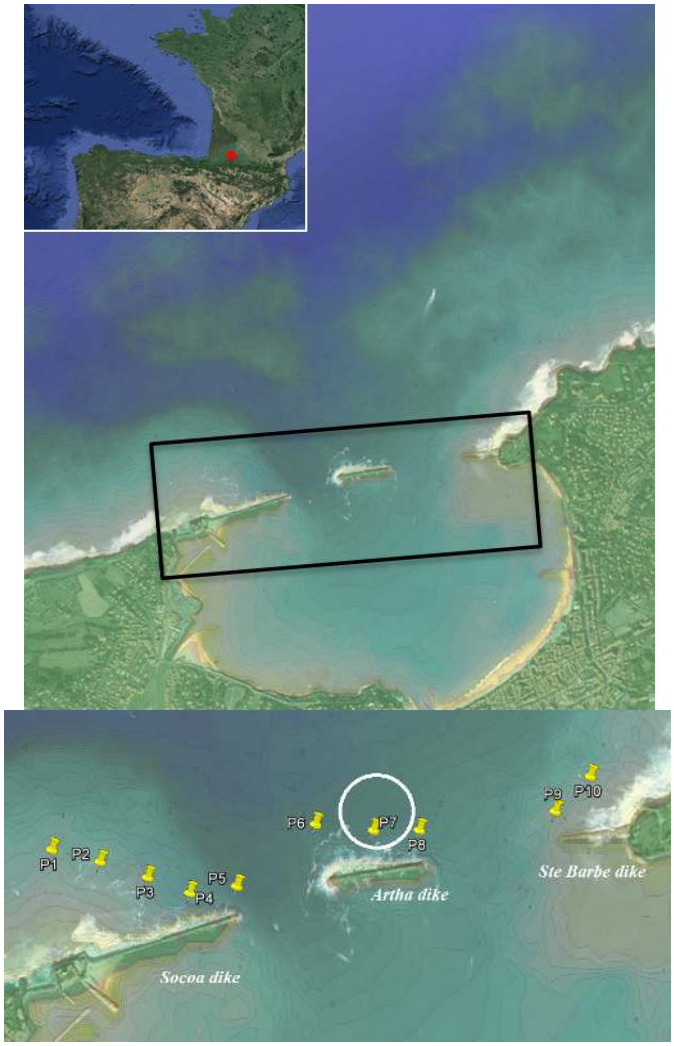

Fig. 1 Saint-Jean-De-Luz breakwaters and wave statistics extraction points (yellow dots).

Fig. 2 Domains of simulations of the SWAN model and locations of the ANEMOC data base points.

Tidal level changes have been also determined over the duration covered by the ANEMOC database using the FES2004 model [11]. With η denoting the water level above the lowest tidal level, the depth in front of the wave converter is $h = h_0 + \eta$.

The wave and tide data set used for estimating the absorbed wave energy by the wave energy converters consists of the water depth h, the significant wave height H_s and the wave period T_p at the position P7. The water depth at P7 is h_0=8m when the tidal level reaches its minimum. Because the time step of the ANEMOC wave data is 1 hour, it was considered that each wave and tide conditions lasted for 1 hour. The 23.5 years of the ANEMOC database corresponds to a total number of 206328 hours.

B. *Wave Climate conditions at the location of wave energy converter*

Fig. 3 shows the probabilities of occurrence of wave conditions at P7 depending on the significant wave height H_s and wave period T_p. Data are plotted in terms of hours per s and per m, the total numbers of hours (206328) corresponding to the duration considered in the ANEMOC data base. Most frequent wave periods are in the range 8s-14s. One can also note that the highest waves correspond with the longest waves.

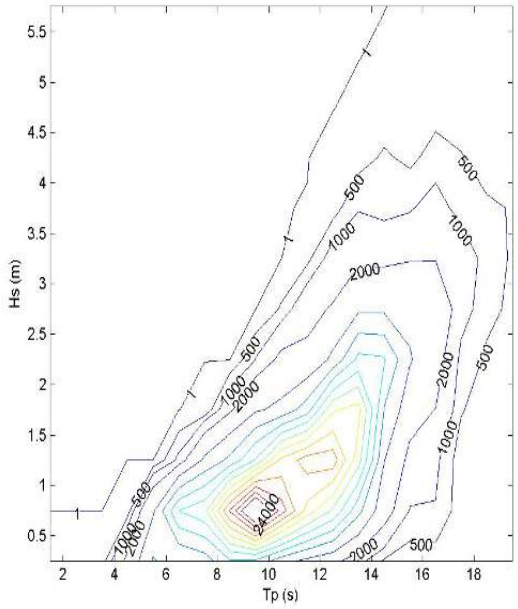

Fig. 3 Wave condition occurrence (in hours) at point P7, depending on the wave period and significant wave height (all tidal levels included)

The probability density function $f(H_s,T_p)$ plotted in Fig. 3 includes all tidal conditions. The probability $f(h,H_s,T_p)$ varies with the water depth h as indicated qualitatively in Table I. It is worth noticing that the wave height is very low for the lowest tidal levels. We may anticipate that energy recovery is negligible for such cases. On the other hand, high H_s occur mainly for high tidal level conditions. The energy recovery has to be considered although such conditions are rare. This dissymmetry is not related to storm surge: the computation of water level variations using the FES2004 model accounts only for the tide. The dissymmetry in the wave height between low and high water levels can be explained by wave breaking dissipation, which is greater at the point P7 for the lowest water levels. Table I shows also that the water depth at point P7 is in the range 9m < h < 12m for 93.9% of conditions, i.e. conditions of very low or very high tidal levels are seldom.

TABLE I
WAVE OCCURRENCE VARIATIONS WITH WATER DEPTH AT POINT P7

h (m)	Occur.	Wave height level
8-8.5m	0.2%	Very low (84% for H_s<1m)
8.5-9m	2.0%	Very low (85% for H_s<1m)
9-9.5m	6.6%	Low (97% for H_s<1.5m)
9.5-10m	13.4%	Low (94% for H_s<1.5m)
10-10.5	17.1%	Low (88% for H_s<1.5m)
10.5-11	19.3%	Mod. (87% for 0.5m<H_s<2.5m)
11-11.5	21.9%	Mod. (90% for 0.5m<H_s<3m)
11.5-12	15.6%	Moderate (95% for 1m<H_s<4m)
12-12.5	3.7%	High (86% for H_s>1.5m)
12.5-13	0.2%	High (97% for H_s>1.5m)

IV. ENERGY RECOVERY USING AN OVERTOPPING WAVE CONVERTER

A. *The SSG principle*

The SSG is an overtopping device (OTD) consisting in a number of reservoirs placed on top of each other, in which the energy of the incoming waves is stored as potential energy. Fig. 4 shows a schematic SSG having 3 reservoirs. The main design parameters are:

- Reservoir crest levels $R_{c,j}$
- Ramp angle α_r
- Front angles θ_j
- Ramp draught d_r
- Horizontal distances between reservoir crests HD_j

The crest heights $R_{c,j}$ are measured in Fig .4 from the lowest tidal level. When the water level changes due to the tide, the actual crest height becomes

$$R'_{c,j}=R_{c,j}-(h-h_0) \quad (1)$$

h is the water depth at the toe of the SSG structure and h_0=8m the water depth at this location for the lowest tidal level.

An SSG system is particularly suitable to install on existing coastal protection, having the advantage to share the costs of installation and maintenance.

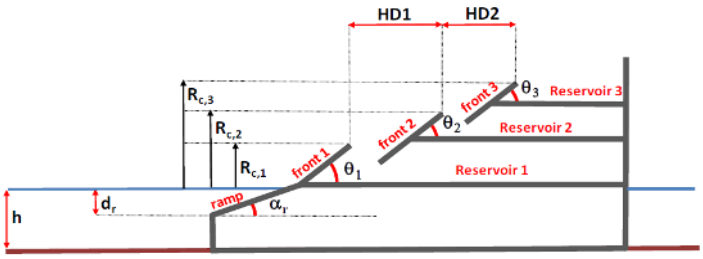

Fig. 4 Sketch of a 3-level SSG structure.

B. Methodology

The efficiency of the SSG system is primarily governed by the flux $q_{ov,j}$ of overtopping water, which enters in each reservoir (labelled with index j). An extensive research has been undertaken for a dozen year [3-6] on the design parameters in order to find relations between SSG design, wave climate and system efficiency. The following equation is used to predict the overtopping flow rate into the j[th] reservoir per unit length of the SSG system

$$q_{ov,j}(H_s,h) = \int_{R_{cj}}^{R_{cj+1}} \frac{dq}{dz} dz = \lambda_j . \sqrt{g.H_s^3} . \frac{A}{B} . \exp\left\{ C . \frac{R'_{c1}}{H_s} \right\} . \exp\left\{ B . \frac{R'_{c,j+1}}{H_s} - B \frac{R'_{c,j}}{H_s} \right\} \quad (2)$$

The overtopping fluxes are distributed in the various reservoirs depending on the choices of wave crest heights $R_{c,j}$. They vary with the significant wave height H_s. The tidal changes are taken into account through the corrected crest height $R'_{c,j}$, as defined by (1).

For the highest reservoir of a device without roof (Fig. 4) $R_{c,j+1}$ is set equal to infinite. Equation (2) has been fitted to experimental data for a standard layout [6] with d_r/h=1, $\alpha_r = \theta_j$=30°-35°, leading to the following set of dimensionless constants: A = 0.197, B = -1.753 and C = -0.408.

It can be noted that neither the wave period nor the wave steepness intervene in equation (2). Various studies [3, 4, 12] have shown that the wave period T_p has an effect on the overtopping volume only if the breaker parameter is low, i.e. $\varepsilon_0 = tg\alpha / \sqrt{L_p / H_s} < 2$. This condition corresponds to spilling waves propagating over a sloping bottom of angle α (L_p is the wavelength). Wave breaking dissipates partly the wave energy, leading to lower wave run-up and weaker overtopping. For this reason, it is recommended to choose a site and a SSG design with enough water at the toe of structure and with a ramp angle high enough, so that $\varepsilon_0 >> 2$ and wave breaking is avoided. For such conditions, waves are surging over the SSG ramp and wave energy dissipation in the run-up process is minimum. The lengths HD_j do not explicitly intervene in (2), which holds subjected that HD_j are chosen appropriately. Experimental studies have shown that the recommended lengths of reservoir openings HD_j varies with the wave period.

Equation (2) integrates a correction factor λ_j which takes into account, as stated by the general formulations of wave run-up and overtopping [11], the effect of roughness, the wave obliquity, the presence of berms, etc. Other parameters have been highlighted by experimental studies [6] like the length of the reservoir mouth, the angle α_r of SSG ramp, the shallow water factor etc. For this study, the correction factors have been ignored, considering the lack of experimental work and validation. It has to be kept in mind that this choice can lead to an over-estimation in energy recovery prediction.

The overtopping volume entering into each reservoir (eq. 2) depends basically on the crest height $R_{c,j}$, the wave height H_s, and the water depth h at the toe of the SSG system.

The power per unit width potentially recovered by reservoir j of the SSG converter for the flow condition (H_s,h) is deduced from the gravity potential energy

$$P_{SSG,j}(H_s,h) = \rho g R'_{c,j} q_{ov,j}(H_s,h) \quad (3)$$

The hydraulic efficiency of reservoir j for the flow condition (H_s,h) is the ratio

$$\eta_{SSG,j} = P_{SSG,j}(H_s,h) / P_{wave}(H_s,h) \quad (4)$$

where P_{wave} is the power flux of incident waves of significant wave height H_s for a water depth h. The averaged power actually recovered by reservoir j of the SSG system is estimated by considering the probability density function $f(h,H_s,T_p)$ at the position P7 as determined in section III

$$P_{recov,j}(H_s,h) = f(H_s,h).\rho g R'_{c,j} . q_{ov,j}(H_s,h) \quad (5)$$

The total energy recovered is the sum of averaged powers, considering all reservoirs and integrating over all tidal levels and significant wave heights. The global hydraulic efficiency is similarly defined

$$\eta_{SSG} = \frac{\sum_j \iint P_{recov,j}(H_s,h) dh\, dH_S}{\iint P_{wave}(H_s,h) f(H_s,h) dh\, dH_S} \quad (6)$$

C. Implementation of a SSG at the Saint-Jean-de-Luz site

A study has been undertaken to determine the optimal crest levels $R_{c,j}$ for a SSG system that may be installed in front of the Artha dike. Iterative computations considering different numbers of reservoirs and varying crest heights have lead to a few conclusions. As expected, increasing the number of reservoirs improves the efficiency. The optimal vertical distance between neighbouring reservoirs seems to be 0.5 m. Nevertheless, building a SSG system having a high number of reservoirs is inappropriate, considering the construction cost and marginal increase in hydraulic efficiency. Three optimal combinations have been selected for a SSG device having 3, 4 and 5 levels reservoirs, respectively. Table II indicates their geometrical parameters, the averaged absorbed power and their respective overall efficiency. The SSG #3 (5 reservoirs) has a hydraulic efficiency of 22.9 %, which is acceptable compared to an optimal solution having ten reservoirs (efficiency 27%). The averaged power recovered by the SSG system is in the order of 3 kW/m at point P7, where the averaged incident wave energy flux is 14.3 kW/m.

TABLE II
ENERGY RECOVERY BY SSG SYSTEMS WITH 3, 4 AND 5 LEVELS RESERVOIRS

# SSG	Nb of reservoir	$R_{c,1}$ (m)	$R_{c,2}$ (m)	$R_{c,3}$ (m)	$R_{c,4}$ (m)	$R_{c,5}$ (m)	P_{recov} (kW/m)	Hydraulic efficiency
1	3	3	4.5	6.75	-	-	2.5	17.5 %
2	4	2.5	4	5	8	-	2.96	20.1 %
3	5	2.5	3.5	4.5	5.5	8	3.27	22.9 %

Table III shows details of the energy recovered by the three reservoirs of SSG #1, versus the significant wave height (upper part of the table) and versus the water depth (lower part of the table). The middle reservoir recovers 46% of the total energy and the lower and upper reservoirs recover 28% and 26% of it, respectively. Most of the recovered energy is the energy of wave with significant wave height in the range 1 to

3m. The highest waves do not contribute much due their scarcities. The SSG design is optimized with a moderate crest height of the upper reservoir. Little energy is recovered at high and low tides. At high tide, the lowest reservoir recovers no energy because it is submerged.

TABLE III
ENERGY RECOVERED BY THE DIFFERENT RESERVOIRS OF THE SSG #1 DEPENDING ON SIGNIFICANT WAVE HEIGHT ON WATER DEPTH (TIDE)

H_s (m) h(m)	Prob. (%)	$P_{moy,R1}$ (kW/m)	$P_{moy,R2}$ (kW/m)	$P_{moy,R3}$ (kW/m)	P_{recov} (kW/m)	Hydraulic eff. (%)
0.25	11.0	0.0002	0.0001	0	0.0003	0.00
0.75	32.5	0.0258	0.0187	0.0002	0.0447	0.31
1.25	23.5	0.0882	0.0932	0.0076	0.189	1.32
1.75	13.9	0.1263	0.1694	0.0364	0.3321	2.32
2.25	8.6	0.1389	0.2202	0.0829	0.442	3.09
2.75	5.0	0.1217	0.22	0.1204	0.4621	3.23
3.25	2.8	0.0916	0.1825	0.1312	0.4053	2.83
3.75	1.5	0.0589	0.1326	0.1171	0.3086	2.16
4.25	0.7	0.0354	0.0852	0.0883	0.2089	1.46
4.75	0.3	0.0163	0.0457	0.0552	0.1172	0.82
5.25	0.1	0.0063	0.019	0.0252	0.0505	0.35
5.75	0.03	0.0013	0.0057	0.0089	0.0159	0.11
TOT.	100	0.7109	1.1923	0.6734	2.58	17.5
8.25	0.2	0.007	0.0039	0.0018	0.0127	0.09
8.75	2.0	0.055	0.0343	0.0159	0.1052	0.74
9.25	6.6	0.1403	0.0933	0.0452	0.2788	1.95
9.75	13.4	0.2142	0.1586	0.0792	0.452	3.16
10.25	17.1	0.181	0.1637	0.0818	0.4265	2.98
10.75	19.3	0.1134	0.2015	0.1023	0.4172	2.92
11.25	21.9	0	0.2823	0.1538	0.4361	3.05
11.75	15.6	0	0.2057	0.1298	0.3355	2.35
12.25	3.7	0	0.049	0.0579	0.1069	0.75
12.75	0.2	0	0	0.0057	0.0057	0.04
TOT.	100	0.7109	1.1923	0.6734	2.58	17.5

Using topographic data of the Artha breakwater, a possible integration of the SSG system #1 (3 reservoirs) in the breakwater is sketched in Fig. 5.

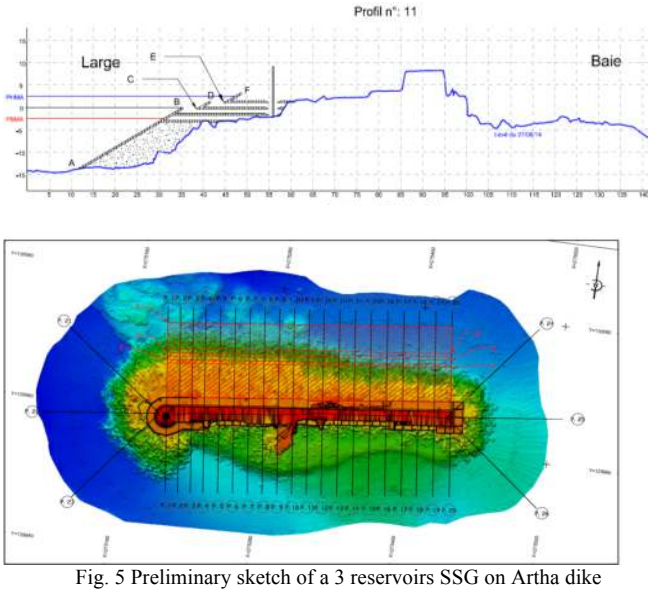

Fig. 5 Preliminary sketch of a 3 reservoirs SSG on Artha dike

D. Discussion

This study gives an estimate of the energy potentially recovered by a SSG system installed in front of the Artha dike and of its overall hydraulic efficiency. The efficiency is probably over-estimated due to the neglected correction factors. As explained in the introduction, other energy losses (water fall, hydraulic turbines and electrical equipment) are not taken account even if estimates are available in the literature [4]. We conclude from Table II that a SSG system at the Artha dike can recover an average annual power of about 3 kW/m, corresponding to an overall hydraulic of efficiency of 21%. The power recovered by a SSG system extending over the full length (250m) of the Artha dike is approx 750 kW in annual average, providing an annual energy production of 6.6 GWh.

To these observations, it has to be noted that power varies with the seasons. During wintertime, the energy can be approximately 5 times higher than in summer time.

V. ENERGY RECOVERY USING A FLAP-TYPE CONVERTER

A. Flap Geometry

The flap is sketched in Fig. 6 and its parameters are given in Table IV. The water depth h at the flap is the only geometrical parameter that varies, due to the tide. When the flap is in the upright position, the water depth at the flap is 8 m and 13 m, respectively for the lowest and highest tidal levels. The flap is fully submerged only in the highest tide conditions.

TABLE IV
FLAP GEOMETRICAL AND MECHANICAL PARAMETERS

Geometrical Parameters		Mechanical Parameters	
h	Water depth at the flap	$6\ 10^4$kg	Flap mass M
11 m	Flap height	3.7310^6	Moment of inertia
20 m	Flap width W	kg m^2	from rotation axis
1.5 m	Flap thickness	5.33 m	d_1: distance of flap
2 m	Height of the pivot above the bottom		centre of gravity from rotation axis

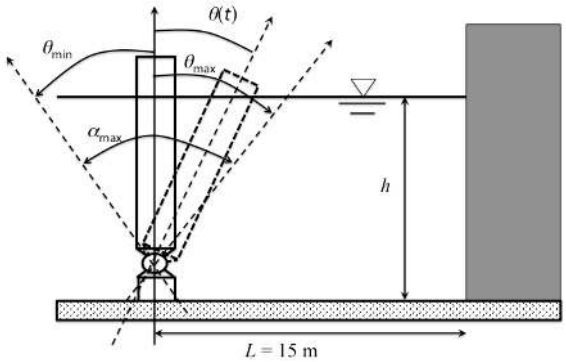

Fig. 6 Flap geometry

B. Methodology

The recovered energy is determined from the balance of angular momentum, which is driven by the torque applied on the flap by the waves. The flap is additionally subjected to the torque applied by the PTO converter and the torque applied by

the radiated waves produced by flap motion. Most important results of the modelling work are highlighted here. The details can be found in [7-8].

The flap motion is given by

$$I_y\ddot{\theta} = \tau_{wave} + \tau_{PTO} + \tau_{rad} - g(\rho V - M)d_1\theta \quad (7)$$

The angle θ, defined in Fig. 6, is θ=0 when the flap is in the upright position and I_y denotes the moment of inertia of the flap about its rotation axis.

A linear Power Take Off converter was chosen, i.e.

$$\tau_{PTO} = -B_{PTO}\dot{\theta} - K_{PTO}\theta \quad (8)$$

During a period of time T the absorbed energy is

$$\int_0^T -\tau_{PTO}(t)\dot{\theta}(t)dt = B_{PTO}\int_0^T \dot{\theta}^2(t)\,dt + K_{PTO}\left\{\theta^2(T) - \theta^2(0)\right\}/2 \quad (9)$$

The damping coefficient B_{PTO} is the main parameter driving the energy recovery. A low B_{PTO} value will not allow recovering significant energy. Conversely, if B_{PTO} is high, the square of the flap angular velocity $\dot{\theta}^2$ will be much decreased, reducing as well the recovered energy. An important issue of this paper is to determine the optimal choice of B_{PTO} depending on the wave conditions.

According to Eq. (9) the stiffness coefficient K_{PTO} contributes to the absorbed energy through the initial and final positions of the flap. This term is then negligible if T is long enough.

The third term in the right hand side of (7) is the torque due to buoyancy (in addition to quantities defined in Table IV ρ is the fluid density and V the submerged volume of the flap). It does not contribute to the absorbed energy when the initial and final angular positions are identical.

The power recovered by the flap for a given water depth h was computed for random waves. A Jonswap spectrum with significant wave height H_s, period T_p and frequency spreading parameter γ=3.3 was used. Thanks to linearity, equations were solved in the frequency domain.

The main terms driving the flap oscillation are the torque applied by the incoming waves $\tau_{wave}(t)$ and the torque applied by the radiated waves $\tau_{rad}(t)$. In the framework of linear wave theory and in the frequency domain

$$\tau_{rad}(t) = -C_M\ddot{\theta} - C_A\dot{\theta} \quad (10)$$

The coefficient $C_M(\omega)$ and $C_A(\omega)$ were determined using the potential wave model AQUAPLUS [13] depending on the wave frequency ω. The computation was performed with the geometry shown in Fig. 6, for which the flap is at a distance L=15 m in front of a reflective wall. The wall increases the recovered energy as discussed later.

The torque $\tau_{wave}(t)$ applied by the incoming waves was also computed using the AQUAPLUS model.

The flow model considers an inviscid fluid. For monochromatic wave conditions, the energy recovered by the converter during a wave period is simply the difference between the energy transmitted to the converter by the torque applied by the incoming waves and the wave energy radiated by the flap oscillation,

$$B_{PTO}\int_0^{T_p}\dot{\theta}^2(t)\,dt = \int_0^{T_p}\tau_{wave}(t)\dot{\theta}(t)dt - C_A\int_0^{T_p}\dot{\theta}^2(t)dt \quad (11)$$

Incorporating (8) and (10), Eq. (7) becomes

$$\left(I_y + C_M\right)\ddot{\theta} + \left(B_{PTO} + C_A\right)\dot{\theta} + \left(K_{PTO} + g(\rho V - M)d_1\right)\theta = \tau_{wave} \quad (12)$$

A linear analysis of Eq. (12) allows identifying a resonance frequency. Nevertheless, the amplitude θ of the flap oscillation is restricted for an obvious geometrical reason and also in order to remain within the framework of linear modelling, which is the basis of the AQUAPUS solver.

The optimal choice of PTO parameters B_{PTO} and K_{PTO}, which is primarily guided by the maximisation of the energy recovered, takes into account amplitude constraints for the flap oscillations. Considering the values of the moment of inertia I_y (Table IV) and of the radiations coefficients is a guide for defining the range of values for the PTO parameters B_{PTO} and K_{PTO}. The optimization study of the PTO parameters was carried out by considering values for B_{PTO} and K_{PTO} in the range 10^6 – 16 10^7 (with their respective units kg.m^2.s^{-1} and kg.m^2.s^{-2}).

As done in section IV for estimating the energy recovery by an overtopping wave converter, the power $P_{flap}(h,H_s,T_p)$ recovered by the flap converter was computed for each wave and tidal condition. The probability of occurrence $f(h,H_s,T_p)$ was determined as the ratio of the number of hours during which the conditions (h,H_s,T_p) occurred at point P7 to the number of hours in the ANEMOC data base (206328). The mean power P_{recov} recovered by the flap converter was then deduced by multiplying the power matrix with the matrix of probability occurrence

$$P_{recov}(h,H_s,T_p) = \Sigma\, P_{flap}(h,H_s,T_p).f(h,H_s,T_p) \quad (13)$$

C. *Wave energy recovery by the flap converter*

The averaged annual power recovered by the converter divided by the flap width is detailed in Table V depending on the water depth. Results are given for two sets of PTO parameters. Firstly, B_{PTO} is optimized for K_{PTO}=2 10^7 kg.m^2.s^{-2}. Then, both B_{PTO} and K_{PTO} are optimized. Optimization aims at maximizing the recovered energy, with the constraint that the flap motion remains in an acceptable range. The selection of PTO parameters is constrained in the following to the condition $-20° < \theta < 20°$. For the frequency domain model operated in random wave conditions, the maximum peak-to-peak angle $\alpha_{max}=\theta_{max}-\theta_{min}$ of flap motion is determined as the average of the ten percent greatest angles of oscillation. A condition of operation for energy recovery is retained if $\alpha_{max}<40°$. Angles definitions are shown in Fig. 6.

Table V indicates that most of the energy is recovered during intermediate tidal levels. The water depth ranges between 9.5 m and 12 m during 87.3% of time. A dissymmetry in the energy recovery is noticed in Table V. It is linked to the wave data distribution at point P7, given in Table I, which shows that the highest wave conditions occur predominantly during high water depth conditions. Wave condition with H_s>4.5m never occurred for h<10.5m, whereas h>12m for 57% of wave conditions having H_s> 5m. The wave energy recovered is larger when the water depth is in the

range 12.5-13.0 m as compared to the range 8-8.5 m. They have the same probability of occurrence (0.2%), but the high wave conditions (H_s> 5m) are too rare (0.14% of occurrence) to provide a significant energy recovery.

TABLE V
ENERGY RECOVERED BY A FLAP CONVERTER DEPENDING ON WATER DEPTH

h (m)	Occur-rence	P_{recov}/W (kW/m) for K_{PTO} = 2 10^7 kg.m^2.s^{-2}	P_{recov}/W (kW/m) for K_{PTO} optimized	Incident wave flux (kW/m)
8-8.5	0.2%	0.010		0.008
8.5-9	2.0%	0.100		0.061
9-9.5	6.6%	0.399		0.222
9.5-10	13.4%	0.997		0.593
10-10.5	17.1%	1.556		1.019
10.5-11	19.3%	2.245		1.769
11-11.5	21.9%	3.534	3.594	3.790
11.5-12	15.6%	3.289	3.344	4.808
12-12.5	3.7%	0.991		1.880
12.5-13	0.2%	0.054		0.135
TOTAL	100%	13.203		14.285

The major conclusion of Table V is that the flap allows recovering a significant amount of energy. The total energy recovered per unit length of the flap is 13.2 kW/m in annual average. The value is only slightly less than the mean incident wave flux at the position P7, which is 14.3 kW/m.

The optimization of PTO parameters is discussed in more detail in the next section. Table V at this stage indicates that optimizing both B_{PTO} and K_{PTO} increases little the amount of energy recovered as compared to the case where only B_{PTO} is optimized and K_{PTO} = 2 10^7 kg.m^2.s^{-2}. Computations for optimizing both B_{PTO} and K_{PTO} were only carried out for the water depth 11.25 m and 11.75 m. A significant part of energy is recovered for these conditions. The comparison indicates that the improvement brought by the optimization of K_{PTO} remains limited.

D. PTO optimization

The optimization of PTO parameters is analysed here for the water depth condition 11.5 m < h < 12 m. 25% of the total wave energy is recovered for this water level (Table V).

Contour plots are presented in Fig. 7 for the absorbed power per unit length and for the maximum amplitude of oscillation of the flap, depending on the values of the PTO parameters. Two wave conditions are considered.

For a greater wave height (Fig. 7a, H_s=2.25m), the choice of optimized PTO values is restricted by the constraint α_{max}<40° on the flap motion amplitude. The maximum power (24.80 kW/m) is recovered for B_{PTO}=7.6 10^7 kg.m^2.s^{-1} and K_{PTO}=2.4 10^7 kg.m^2.s^{-2} and the corresponding maximum amplitude is α_{max}=40°. The flap dynamics is driven by a resonance like phenomena. The PTO parameters are chosen in order to take advantage of it for recovering as much energy as possible, while limiting the flap motion amplitude within the required range. The power surface $P_{flap}(B_{PTO}, K_{PTO})$ is smooth. Varying the PTO parameters around the optimized values reduces little the recovered power (still keeping the oscillation in the range -20°<θ<20°). This explains, as observed in Table V, why the energy recovered when both B_{PTO} and K_{PTO} are optimized is only 2% greater than the energy recovered when only B_{PTO} is optimized and K_{PTO} = 2 10^7 kg.m^2.s^{-2}.

For wave heights H_s>1 m, the optimisation of PTO parameters were always obtained with the maximum angular oscillation α_{max}=40°, except a few cases with wave period less than 10s. Fig. 7a is a representative picture for the optimisation of PTO parameters for the wave conditions at St Jean de Luz.

A different pattern is shown in Fig. 7b for a low wave height (H_s=0.25 m) and smaller wave period. The maximum power (0.81 kW/m) is recovered for B_{PTO}=1.6 10^7 kg.m^2.s^{-1} and K_{PTO}=3.2 10^7 kg.m^2.s^{-2} and the maximum amplitude of flap motion is 14.6°. Nevertheless, wave with significant wave heights H_s<1 m do not lead to significant energy (Table VI).

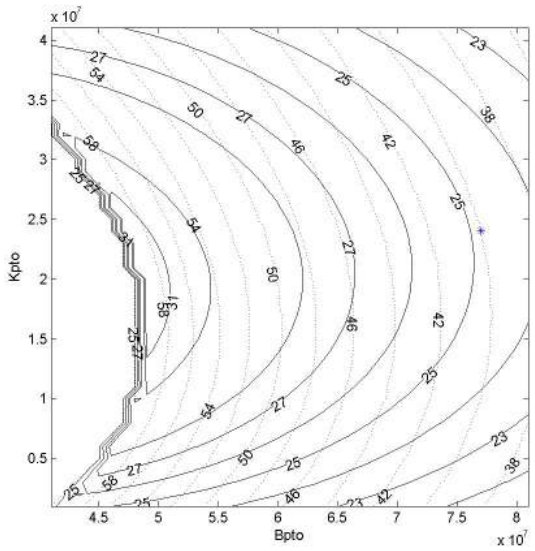

a.

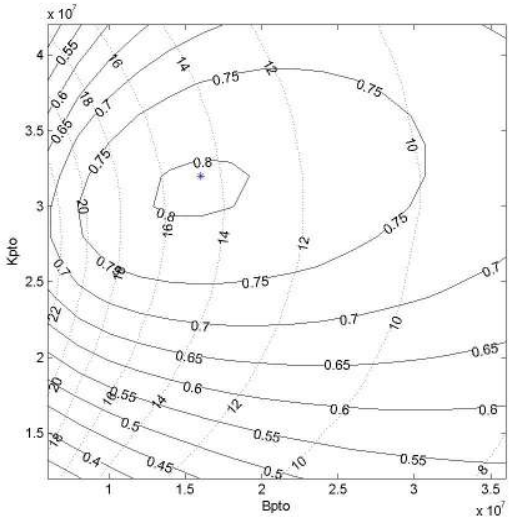

b.

Fig. 7 Contour plots of the power recovered per unit length (solid lines) and of the maximum angle of oscillation (dotted lines) of the flap converter, depending on PTO parameters.
Conditions : h=11.75m ; a: H_s=2.25m, T_p=13.5s ; b: H_s=0.25m, T_p=10.5s.
* indicates the optimized PTO parameters.

In summary, the choice of PTO parameters is imposed by the limitation of the flap motion amplitude for the highest waves. It was chosen to limit the flap motion amplitude below 40°. This constraint is released for small waves and the PTO parameters simply maximize the energy recovery.

TABLE VI
ENERGY RECOVERED BY A FLAP CONVERTER DEPENDING ON THE SIGNIFICANT WAVE HEIGHT AND ON THE WAVE PERIOD
(RESULT GIVEN FOR WATER DEPTH 11.75M)

H_s (m) / T_p (s)	Prob.	Inc. Ener. (kW/m)	Ener. Rec. (kW/m) K_{PTO} fixed	Ener. Rec. (kW/m) K_{PTO} opti.
0.25	2.80%	0.001	0.002	0.002
0.75	1.56%	0.045	0.087	0.098
1.25	2.76%	0.236	0.358	0.381
1.75	3.02%	0.524	0.583	0.598
2.25	2.95%	0.865	0.705	0.713
2.75	2.32%	1.029	0.652	0.654
3.25	1.38%	0.864	0.436	0.437
3.75	0.76%	0.639	0.265	0.258
4.25	0.35%	0.432	0.147	0.149
4.75	0.13%	0.177	0.053	0.053
5.25	0.03%	0.050	0.013	0.013
5.75	0.00%	0.000	0.000	0.000
TOT.	15.5%	4.808	2.289	2.344
9.5s	0.81%	0.069	0.133	0.151
10.5s	1.10%	0.136	0.222	0.237
11.5s	1.46%	0.245	0.320	0.327
12.5s	2.15%	0.477	0.489	0.492
13.5s	2.80%	0.814	0.648	0.650
14.5s	2.11%	0.767	0.484	0.486
15.5s	1.49%	0.659	0.335	0.329
16.5s	1.37%	0.727	0.302	0.302
17.5s	0.70%	0.437	0.151	0.151
18.5s	0.37%	0.228	0.068	0.069
19.5s	0.30%	0.210	0.051	0.053

Table VI gathers the energy recovered by the flap for the water depth h=11.75 m. This condition is an important one as 25% of the averaged power is recovered for this water depth, while its probability of occurrence is 15.5%. The results are given when only B_{PTO} is optimized (K_{PTO} = 2 10^7 kg.m^2.s^{-2}) and when K_{PTO} and B_{PTO} are both optimized. Optimizing both K_{PTO} and B_{PTO} increases by about 2% the amount of energy recovered as compared to the case when only B_{PTO} is optimized. The energy recovered, expressed as the mean power per unit width of the flap, is detailed in the upper part of Table VI versus the wave height (integrating over all wave periods) and, in the lower part, versus the wave periods (integrating over all wave heights). Most of the energy recovered is due to waves having the wave height in the range 1m < H_s < 3.5m. The highest waves (H_s > 5m) are too scarce to provide significant energy recovery. The lowest waves conditions (H_s < 1m) are more frequent but their energy is small. The results are similar to those obtained for the wave overtopping converter (Table III). One also notice that the energy recovered correspond to waves having the period in the range 11s < T_p < 17s. Waves with period less than 9s are not included in the lower part of Table VI since their contribution is negligible.

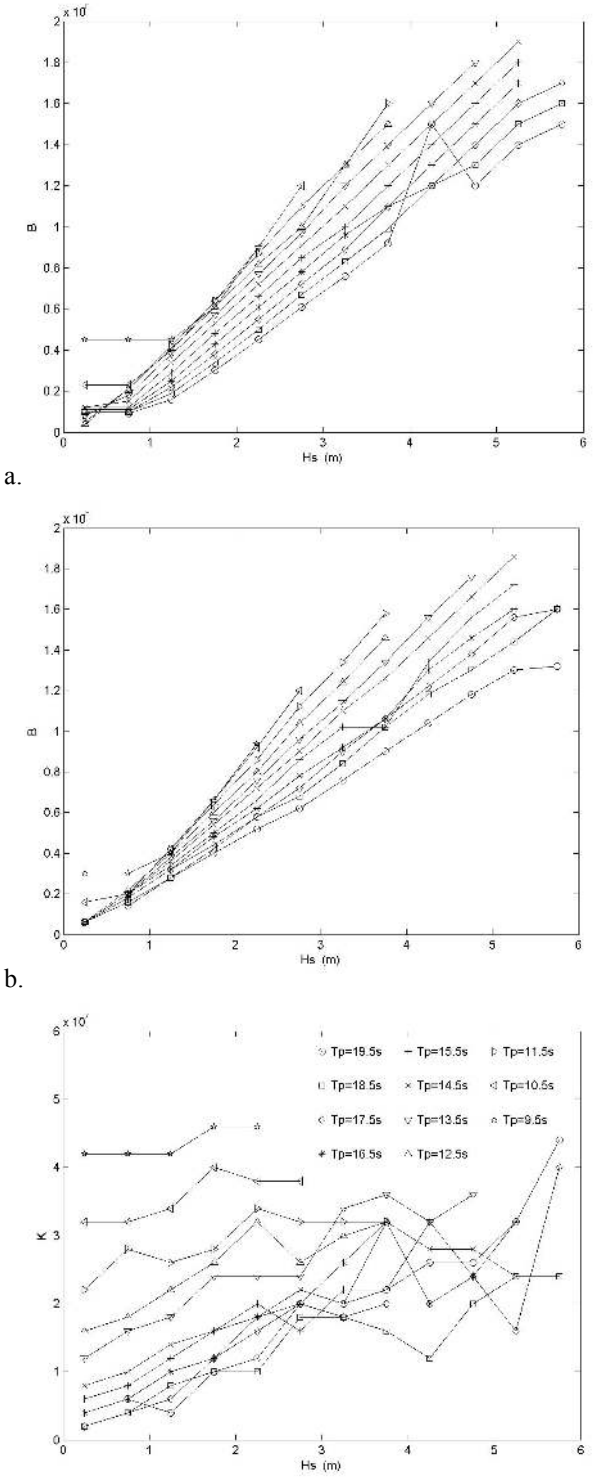

Fig. 8 Variations of PTO parameters with significant wave height H_s, depending on the wave period T_p. Computation for h=11.75m ; a: optimized B_{PTO} for K_{PTO} = 2 10^7 kg.m^2.s^{-2} ; b and c : B_{PTO} for K_{PTO} both optimized.

The absorption of energy varies with the wave period. The flap captures about twice the energy of incident waves of short periods (9-12s) along a wave crest of length equal to the flap width, whereas the absorbed power is roughly a quarter of the incident power for long wave periods (18-20s). The point

absorber theory [14] shows that WEC of small size compared to the wavelength can absorb an amount of energy larger than the flux across a wave crest length equal to the flap width. For the present case, the idealized geometry with a reflective wall behind the flap (Fig. 6) influences also the energy recovery.

The adjustment of PTO parameters to the wave conditions is desirable for maximizing the energy recovery. It is also mandatory for limiting the flap motions to an acceptable range. Fig. 8 shows the variations of optimized PTO values with the significant wave height and with the wave period. The case where only B_{PTO} is optimized (K_{PTO} = 2 10^7 kg.m^2.s^{-2}) is first considered (Fig. 8a). Figs. 8b-c then displays the variations of the optimized values of B_{PTO} and K_{PTO} with H_s and T_p. Fig. 8a-b display similar variations of the parameter B_{PTO}, confirming that optimizing K_{PTO} is a secondary goal. As expected, increasing B_{PTO} in relation to increasing wave height is required. The increase is by an order magnitude of 20 for covering the wave height range 0 – 6m. A peculiar behaviour is noticed for small wave periods (9.5s, 10.5s and 11.5s) and low wave heights, because for such conditions, the optimisation of PTO parameters is no longer constrained by the angular requirement α<40°. Nevertheless, little energy is recovered for these conditions.

As mentioned before, the torque applied on the flap is computed assuming an inviscid fluid. The values of energy recovered by the flap given in this paper should therefore be considered as preliminary and additional computations should be done to estimate the reduction in the energy recovered when viscous effects are accounted for. The numerical code has an extension which solves in the time domain the equations presented in section V,*B*. Effect of viscosity is taken into account using a semi-empirical approach (Morison-like damping term). Complementary computations in the time domain, with and without viscous effects, were achieved, considering the representative random wave conditions investigated in Fig. 7a (H_s=2.25m, T_p=13.5s, h=11.75 m). A maximum energy recovery of 24.9 kW/m was obtained for the PTO parameters values K_{PTO}=2.3 10^7kg.m^2.s^{-1} and B_{PTO}=7.6 10^7kg.m^2.s^{-1}. Estimates for the energy recovered and the maximum angle of oscillation of the flap are in agreement with the former computations in the frequency domain. When viscous effects were taken into account, for the same values of PTO parameters, the energy recovery was found to be 18.2 kW/m and the corresponding angular variations were in the range -22°<θ<20°. The reduction due the viscous terms is by 27%. This estimate is in agreement with results given in [15].

These results highlight the need for taking account the viscous effects for computing the torque applied on the flap. The prediction in this paper (Table V) of an energy recovery by the flap of 13.2 kW/m certainly overestimates the recover that the flap can achieve. The values of PTO parameters should be re-optimized in course of computations with viscous effects. In view of estimates given above, we may guess that the averaged power recovered by the activated flap will range between 6 and 9 kW/m, when optimizing the PTO parameters and taking into account viscous effects.

VI. Conclusion

Estimates of energy recovery by the overtopping converter (SSG) and by the flap converter were made for the same wave and tidal forcing, which is determined from real data. The energy recovered is the product of the power matrix for varying wave and tide conditions with the probability matrix of their occurrence. The study shows that the highest waves provide little energy. The main contribution to energy absorption is due to waves of intermediate heights (H_s in the range 1 to 3 m), which are the most frequent. To this end, the two WEC's show a similar response.

The average wave energy flux is high in front of the Artha dike (14.3 kW/m) in Saint Jean de Luz (France). Designs are presented in this paper for a SSG overtopping wave energy converter and for a flap activated wave energy converter. The estimated energy recovered by a SSG system with five reservoirs and crest heights ranging from 2.5 m to 8 m above the lowest tidal level is 3.27 kW per meter of device in annual average. The flap converter is 20 m wide and its height is such that it is entirely submerged only for the highest tidal level. The optimization of the flap converter is driven by the choice of PTO parameters in order to maximize the energy recovery and to keep the maximum flap motion amplitude α_{max} below a given value. The control strategy is part of the technology of the flap activated converter and the choice of the limiting value for α_{max} is critical. A maximum angle α_{max}<40° was chosen. For the wave conditions at St Jean de Luz, our study shows that the optimization of PTO parameters of the flap is primarily driven by the choice of α_{max}. For wave conditions providing significant energy recovery, the optimized values of K_{PTO} and B_{PTO} were always obtained with α_{max}=40°. The value of B_{PTO} has to be increased by a factor of 20 when the wave height is increased from 0.25m to 5.75m. The optimisation of K_{PTO} does not improve the energy recovery, as long as B_{PTO} can be adjusted to maintain the oscillation with the admitted angular range. Computations in the frequency domain, which neglect viscous effects, lead to an estimate of the energy recovered by the flap for all waves and tidal conditions of 13.2 kW/m. Complementary computations for selected cases indicate that viscous effects reduce by about on third the amount of energy recovered. In view of these results we anticipate an averaged power recovered by the activated flap between 6 and 9 kW/m. This estimate is a matter of discussion between the authors. The given estimates are preliminary. They will checked in future by further computations.

The knowledge of wave converters systems is enriched by the comparison between them, and we hope that our paper contribute to it. Comparing an SSG overtopping WEC and a flap WEC is nevertheless not that easy, when the comparison is attached to a site. For the 250 m long Artha dike at Saint Jean de Luz, expressing the energy recovered per unit length of a SSG system makes sense if the dike can be entirely equipped with it. On the other hand, expressing the energy recovered by a flap per unit flap length is more difficult. The flap is an individual device, eventually part of a wave farm in front of the dike. We may in general observe that the spacing

between neighbouring flaps is of the order of the flap width [16]. The total energy recovered by the wave farm should be optimized and the result will certainly not be given in term of the power captured by unit length of the flap or per unit length of the dike.

The SSG system is a passive wave converter, whereas the flap is an active converter. It is expected that an active WEC can recover more energy than a passive WEC, if the parameters of the active WEC are driven in an appropriate manner, but control will also have an additional cost. The comparison between the two WEC should then be considered through a Levelized Cost of Energy (LCOE) analysis that will include the losses due to electrical converters, turbines etc, and the additional cost of control for an active WEC. The comparison between the two converters should finally consider civil engineering work for installing the converters, investment and operating costs, and finally the consequences regarding environmental impacts and the efficiency of protection for the bay.

ACKNOWLEDGMENT

Partial financial support by the EMACOP national program (France) and by the Conseil Général des Pyrénées Atlantiques (authority in charge of coastal structures at St Jean de Luz) is acknowledged.

REFERENCES

[1] A.F.O. Falcão, "Modelling of wave energy conversion," Int. Report Instituto Superior Técnico, UniversidadeTécnica de Lisboa, 2014.

[2] Y. Torre-Enciso, I Ortubia, L.I. López de Aguileta and J. Marqués, "Mutriku wave power plant: from the thinking out to the reality," in *Proc. EWTEC2009*, 2009, pp. 319-329.

[3] J.P. Kofoed, "Wave overtopping of marine structures – Utilisation of wave energy," PhD thesis, Aalborg University, Dec. 2002.

[4] L. Margheritini, "R&D toward commercialization of the Sea wave Slot cone Generator (SSG) overtopping wave energy converter," PhD thesis, Aalborg University, Nov. 2009.

[5] P. Meinert, L.Gilling and J.P. Kofoed, "User manual for SSG power simulation 2," Int. report, Aalborg University, June 2006.

[6] D. Vinicianza, L. Margheritini, J.P. Kofoed, and M.Buccino, "The SSG Wave Energy converter : performance, status and recent developments," *Energies*, vol. 5, pp. 193-226, 2012.

[7] M. Folley, T.W.T. Whittaker and J. van't Hoff, "The design of small seabed-mounted bottom-hinged wave energy converters," in *Proc. EWTEC2007*, 2007.

[8] V. Baudry, "Rapport d'étude EMACOP : Développement d'un outil d'évaluation du rendement des dispositifs de type batteur inverse," 2014.

[9] http://www.swan.tudelft.nl/

[10] http://anemoc.cetmef.developpement-durable.gouv.fr

[11] http://www.legos.obs-mip.fr/produits/soa/niveau-de-la-mer/maree/modele-global-de-maree-fes

[12] J.W. Van der Meer and J.P.F.M. Janssen, "Wave run up and wave overtopping at dikes". In *Wave Forces on Inclined and Vertical Wall Structures*; Kobayashi, N., Demirbilek, Z., Eds.; American Society of Civil Engineers (ASCE) Publications: Reston, VA, USA, pp. 1–27, 1995.

[13] G. Delhommeau, "Seakeeping codes in aquadyn and aquaplus,", in *Proc.19th WEGEMT School, numerical simulation of hydrodynamics, ships and offshore structures*, 1993.

[14] D.V. Evans, "A theory for wave-power absorption by oscillating bodies, " *J. Fluid Mech.*, vol. 77, part 1, pp. 1-25, 1976.

[15] A. Babarit, J. Hals, A. Kurniawan, M. Muliawan, T. Moan and J. Krostad, "Numerical estimation of energy delivery from a selection of wave energy converters," Final report of the NumWEC project, Int. Report Ecole Centrale de Nantes (France), Centre for Ships and Ocean Structures and Statkraft (Norway), December 2011.

[16] D. Sarkar, E. Renzi and F. Dias, "Wave farm modelling of oscillating wave surge converters," *Proc. R. Soc. A*, 470(2167), p. 20140118, 2014.